

# Spontaneous decay dynamics in atomically doped carbon nanotubes

I. V. Bondarev\* and Ph. Lambin

*Facultés Universitaires Notre-Dame de la Paix, 61 rue de Bruxelles, 5000 Namur, BELGIUM*

We report a strictly non-exponential spontaneous decay dynamics of an excited two-level atom placed inside or at different distances outside a carbon nanotube (CN). This is the result of strong non-Markovian memory effects arising from the rapid variation of the photonic density of states with frequency near the CN. The system exhibits vacuum-field Rabi oscillations, a principal signature of strong atom-vacuum-field coupling, when the atom is close enough to the nanotube surface and the atomic transition frequency is in the vicinity of the resonance of the photonic density of states. Caused by decreasing the atom-field coupling strength, the non-exponential decay dynamics gives place to the exponential one if the atom moves away from the CN surface. Thus, atom-field coupling and the character of the spontaneous decay dynamics, respectively, may be controlled by changing the distance between the atom and CN surface by means of a proper preparation of atomically doped CNs. This opens routes for new challenging nanophotonics applications of atomically doped CN systems as various sources of coherent light emitted by dopant atoms.

PACS numbers: 61.46.+w, 73.22.-f, 73.63.Fg, 78.67.Ch

## I. INTRODUCTION

It has long been recognized that the spontaneous emission rate of an excited atom is not an immutable property, but that it can be modified by the atomic environment. Generally called the Purcell effect [1], the phenomenon is qualitatively explained by the fact that the local environment modifies the strength and distribution of the *vacuum* electromagnetic modes with which the atom can interact, resulting indirectly in the alteration of atomic spontaneous emission properties.

The Purcell effect took on special significance recently in view of rapid progress in physics of nanostructures. Here, the control of spontaneous emission has been predicted to have a lot of useful applications, ranging from the improvement of existing devices (lasers, light emitting diodes) to such nontrivial functions as the emission of nonclassical states of light [2]. In particular, the enhancement of the spontaneous emission rate can be the first step towards the realization of a thresholdless laser [3] or a single photon source [4]. The possibility to control atomic spontaneous emission was shown theoretically for microcavities and microspheres [5, 6, 7], optical fibers [8], photonic crystals [9], semiconductor quantum dots [10]. Recent technological progress in the fabrication of low-dimensional nanostructures has enabled the experimental investigation of spontaneous emission for microcavities [11], photonic crystals [12], quantum dots [13].

Carbon nanotubes (CNs) are graphene sheets rolled-up into cylinders of approximately one nanometer in diameters. Extensive work carried out worldwide in recent years has revealed the intriguing physical properties of these novel molecular scale wires [14, 15]. Nanotubes have been shown to be useful for miniaturized

electronic, mechanical, electromechanical, chemical and scanning probe devices and materials for macroscopic composites [16]. Important is that their intrinsic properties may be substantially modified in a controllable way by doping with extrinsic impurity atoms, molecules and compounds [17]. This opens routes for *new* challenging nanophotonics applications of atomically doped CN systems as various sources of coherent light emitted by dopant atoms. Recent successful experiments on encapsulation of single atoms into single-wall carbon nanotubes [18] and their intercalation into single-wall CN bundles [17, 19] stimulate an analysis of atomic spontaneous emission in such systems as a first step towards their nanophotonics applications.

Typically, there may be two qualitatively different regimes of interaction of an atomic excited state with a vacuum electromagnetic field in the vicinity of the CN. They are the weak coupling regime and the strong coupling regime [20]. The former is characterized by the monotonous exponential decay dynamics of the upper atomic state with the decay rate altered compared with the free-space value. The latter is, in contrast, strictly non-exponential and is characterized by reversible Rabi oscillations where the energy of the initially excited atom is periodically exchanged between the atom and the field. In the present paper, we develop the quantum theory of the spontaneous decay of an excited two-level atom near a CN and derive the evolution equation of the upper state of the system. By solving it numerically, we demonstrate the strictly non-exponential spontaneous decay dynamics in the case where the atom is close enough to the CN surface. In certain cases, the system exhibits vacuum-field Rabi oscillations — a result already detected for quasi-2D excitonic and intersubband electronic transitions in semiconductor quantum microcavities [21, 22] and never reported for atomically doped CNs so far.

The rest of the paper is arranged as follows. Section II presents a theoretical model we use to derive the evolution equation of the upper state population probability

---

\*On leave from the Institute for Nuclear Problems at the Belarusian State University, Bobruiskaya Str.11, 220050 Minsk, BELARUS

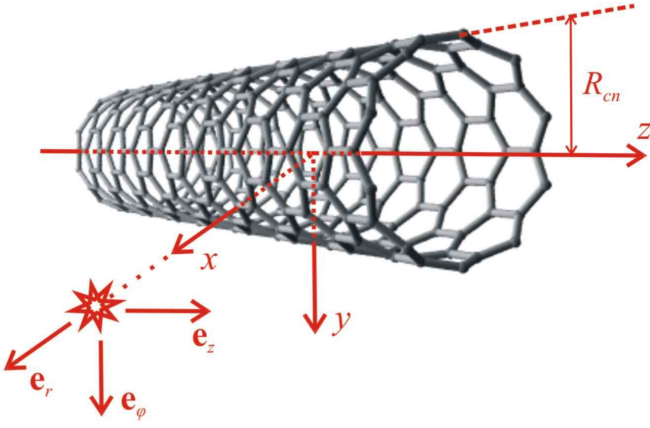


FIG. 1: (Color online) The geometry of the problem.

amplitude of the composed quantum system "a two-level atom interacting with a quantized CN-modified vacuum radiation field". In describing atom-field interaction we follow the original line of Refs. [5, 6], adopting their electromagnetic field quantization scheme for a particular case of the field near an infinitely long achiral single-wall CN. The carbon nanotube is considered as an infinitely thin anisotropically conducting cylinder. Its surface conductivity is represented in terms of the  $\pi$ -electron dispersion law obtained in the tight-binding approximation with allowance made for azimuthal electron momentum quantization and axial electron momentum relaxation [23]. Only the axial conductivity is taken into account and the azimuthal one, being strongly suppressed by transverse depolarization fields [24, 25, 26, 27], is neglected. In Section III, the time dynamics of the upper state population probability is analyzed qualitatively in terms of two different approximations admitting analytical solutions of the evolution equation derived in Section II. They are the Markovian approximation and the single-resonance approximation of the density of photonic states in the vicinity of the CN. Section IV presents and discusses the results of the numerical solution of the evolution equation for various particular cases where the atom is placed in the center and near the wall inside, and at different distances outside achiral CNs of different radii. A summary and conclusions of the work are given in Section V.

## II. THE MODEL

The quantum theory of the spontaneous decay of excited atomic states in the presence of the CN involves an electromagnetic field quantization procedure. Such a procedure faces difficulties similar to those in quantum optics of 3D Kramers-Kronig dielectric media where the canonical quantization scheme commonly used does not work since, because of absorption, corresponding operator Maxwell equations become non-Hermitian [28]. As a

result, their solutions cannot be expanded in power orthogonal modes and the concept of modes itself becomes more subtle. We, therefore, use an alternative quantization scheme developed in Refs. [5, 6], where the Fourier-images of electric and magnetic fields are considered as quantum mechanical observables of corresponding electric and magnetic field operators. The latter ones satisfy the Fourier-domain operator Maxwell equations modified by the presence of a so-called operator noise current density  $\hat{\mathbf{J}}(\mathbf{r}, \omega)$  written in terms of a 3D vector bosonic field operator  $\hat{\mathbf{f}}(\mathbf{r}, \omega)$  and a medium dielectric tensor  $\epsilon(\mathbf{r}, \omega)$  (supposed to be diagonal) as

$$\hat{\mathbf{J}}_i(\mathbf{r}, \omega) = \frac{\omega}{2\pi} \sqrt{\hbar \text{Im} \epsilon_{ii}(\mathbf{r}, \omega)} \hat{f}_i(\mathbf{r}, \omega), \quad i = 1, 2, 3. \quad (1)$$

This operator is responsible for correct commutation relations of the electric and magnetic field operators in the presence of medium-induced absorption. In this formalism, the electric and magnetic field operators are expressed in terms of a continuum set of the 3D vector bosonic fields  $\hat{\mathbf{f}}(\mathbf{r}, \omega)$  by means of the convolution over  $\mathbf{r}$  of the current (1) with the *classical* electromagnetic field Green tensor of the system. The bosonic field operators  $\hat{\mathbf{f}}^\dagger(\mathbf{r}, \omega)$  and  $\hat{\mathbf{f}}(\mathbf{r}, \omega)$  create and annihilate single-quantum electromagnetic medium excitations. They are defined by their commutation relations and play the role of the fundamental dynamical variables in terms of which the Hamiltonian of the composed system "electromagnetic field + dissipative medium" is written in a standard secondly quantized form as

$$\hat{H} = \int d\mathbf{r} \int_0^\infty d\omega \hbar \omega \hat{\mathbf{f}}^\dagger(\mathbf{r}, \omega) \cdot \hat{\mathbf{f}}(\mathbf{r}, \omega). \quad (2)$$

Consider a two-level atom positioned at an arbitrary point  $\mathbf{r}_A$  near the CN. Since the problem has a cylindrical symmetry, it is convenient to assign the orthonormal cylindric basis  $\{\mathbf{e}_r, \mathbf{e}_\varphi, \mathbf{e}_z\}$  in such a way that  $\mathbf{r}_A = r_A \mathbf{e}_r = \{r_A, 0, 0\}$  and  $\mathbf{e}_z$  is directed along the nanotube axis (see Figure 1). Let the atom interact with a quantized electromagnetic field via an electric dipole transition of frequency  $\omega_A$ . The atomic dipole moment may be assumed to be directed along the CN axis,  $\mathbf{d} = d_z \mathbf{e}_z$ . The contribution of the transverse dipole moment orientation is suppressed because of strong depolarization of the transverse field in an isolated CN [24, 25, 26, 27]. Strong transverse depolarization along with transverse electron momentum quantization allow one to neglect the azimuthal current and radial polarizability [23], in which case the dielectric tensor components  $\epsilon_{rr}$  and  $\epsilon_{\varphi\varphi}$  are identically equal to unit. The component  $\epsilon_{zz}$  is caused by the CN longitudinal polarizability and is responsible for the axial surface current parallel to the  $\mathbf{e}_z$  vector. This current may be represented in terms of the 1D bosonic field operators by analogy with Eq. (1). Indeed, taking into account the dimensionality conservation in passing from bulk to a monolayer in Eq. (2) and using a simple

Drude relation [24]

$$\sigma_{zz}(\mathbf{R}, \omega) = -i\omega \frac{\epsilon_{zz}(\mathbf{R}, \omega) - 1}{4\pi S \rho_T}, \quad (3)$$

where  $\mathbf{R} = \{R_{cn}, \phi, Z\}$  is the radius-vector of an arbitrary point of the CN surface,  $R_{cn}$  is the radius of the CN,  $\sigma_{zz}(\mathbf{R}, \omega)$  is the CN surface axial conductivity per unit length,  $S$  is the area of a single nanotube,  $\rho_T$  is the tubule density in a bundle, one immediately has from Eq. (1)

$$\hat{\mathbf{J}}(\mathbf{R}, \omega) = \sqrt{\frac{\hbar \omega \text{Re} \sigma_{zz}(\mathbf{R}, \omega)}{\pi}} \hat{f}(\mathbf{R}, \omega) \mathbf{e}_z \quad (4)$$

with  $\hat{f}(\mathbf{R}, \omega)$  being the 1D bosonic field operator defined on the CN surface. The total Hamiltonian of the system under consideration is then written in terms of  $\hat{f}^\dagger(\mathbf{R}, \omega)$  and  $\hat{f}(\mathbf{R}, \omega)$  operators as

$$\begin{aligned} \hat{\mathcal{H}} = & \int d\mathbf{R} \int_0^\infty d\omega \hbar \omega \hat{f}^\dagger(\mathbf{R}, \omega) \hat{f}(\mathbf{R}, \omega) + \frac{1}{2} \hbar \omega_A \hat{\sigma}_z \\ & - [\hat{\sigma}^\dagger \hat{E}_z^{(+)}(\mathbf{r}_A) d_z + \text{h.c.}] \end{aligned} \quad (5)$$

Here, the three terms represent the electromagnetic field modified by the presence of the CN, the two-level atom and their interaction (within the framework of electric dipole, and rotating wave approximations [5]), respectively. The Pauli operators  $\hat{\sigma}_z = |u\rangle\langle u| - |l\rangle\langle l|$ ,  $\hat{\sigma} = |l\rangle\langle u|$ ,  $\hat{\sigma}^\dagger = |u\rangle\langle l|$  describe the two-level atomic subsystem where  $|u\rangle$  and  $|l\rangle$  are the upper and lower atomic states, respectively. The operators  $\hat{\mathbf{E}}^{(\pm)}(\mathbf{r}_A)$  represent the electric field the atom interacts with. For an arbitrary  $\mathbf{r} = \{r, \varphi, z\}$ , they are defined as follows

$$\hat{\mathbf{E}}(\mathbf{r}) = \hat{\mathbf{E}}^{(+)}(\mathbf{r}) + \hat{\mathbf{E}}^{(-)}(\mathbf{r}),$$

$$\hat{\mathbf{E}}^{(+)}(\mathbf{r}) = \int_0^\infty \hat{\mathbf{E}}(\mathbf{r}, \omega) d\omega, \quad \hat{\mathbf{E}}^{(-)}(\mathbf{r}) = [\hat{\mathbf{E}}^{(+)}(\mathbf{r})]^\dagger. \quad (6)$$

Here,  $\hat{\mathbf{E}}(\mathbf{r}, \omega)$  satisfies the Fourier-domain Maxwell equations

$$\begin{aligned} \nabla \times \hat{\mathbf{E}}(\mathbf{r}, \omega) &= ik \hat{\mathbf{H}}(\mathbf{r}, \omega), \\ \nabla \times \hat{\mathbf{H}}(\mathbf{r}, \omega) &= -ik \hat{\mathbf{E}}(\mathbf{r}, \omega) + \frac{4\pi}{c} \hat{\mathbf{J}}(\mathbf{r}, \omega), \end{aligned} \quad (7)$$

where  $\hat{\mathbf{H}}(\mathbf{r}, \omega)$  stands for the magnetic field operator [defined by analogy with Eq. (6)],  $k = \omega/c$ , and

$$\hat{\mathbf{J}}(\mathbf{r}, \omega) = \int d\mathbf{R} \delta(\mathbf{r} - \mathbf{R}) \hat{\mathbf{J}}(\mathbf{R}, \omega) = 2\hat{\mathbf{J}}(R_{cn}, \varphi, z, \omega) \delta(r - R_{cn}) \quad (8)$$

is the exterior operator current density [with  $\hat{\mathbf{J}}(\mathbf{R}, \omega)$  defined by Eq. (4)] associated with the presence of the CN.

From Eqs. (7) and (8) in view of Eq. (4), it follows that

$$\hat{\mathbf{E}}(\mathbf{r}, \omega) = i \frac{4\pi}{c} k \int d\mathbf{R} \mathbf{G}(\mathbf{r}, \mathbf{R}, \omega) \cdot \hat{\mathbf{J}}(\mathbf{R}, \omega) \quad (9)$$

[and  $\hat{\mathbf{H}} = (ik)^{-1} \nabla \times \hat{\mathbf{E}}$  accordingly], where  $\mathbf{G}(\mathbf{r}, \mathbf{R}, \omega)$  is the Green tensor of the *classical* electromagnetic field in the vicinity of the CN. Its components satisfy the equation

$$\sum_{\alpha=r, \varphi, z} (\nabla \times \nabla \times - k^2)_{z\alpha} G_{\alpha z}(\mathbf{r}, \mathbf{R}, \omega) = \delta(\mathbf{r} - \mathbf{R}), \quad (10)$$

together with the radiation conditions at infinity and the boundary conditions on the CN surface. The Hamiltonian (5) along with Eqs. (6)–(10) and (4) is the modification of the Jaynes–Cummings model [28] for an atom in the vicinity of a solitary CN. The classical electromagnetic field Green tensor of this system is derived in Appendix A.

When the atom is initially in the upper state and the field subsystem is in vacuum, the time-dependent wave function of the whole system can be written as

$$|\psi(t)\rangle = C_u(t) e^{-i(\omega_A/2)t} |u\rangle |\{0\}\rangle$$

$$+ \int d\mathbf{r} \int_0^\infty d\omega C_l(\mathbf{r}, \omega, t) e^{-i(\omega - \omega_A/2)t} |l\rangle |\{1(\mathbf{r}, \omega)\}\rangle, \quad (11)$$

where  $|\{0\}\rangle$  is the vacuum state of the field subsystem,  $|\{1(\mathbf{r}, \omega)\}\rangle$  is its excited state where the field is in a single-quantum Fock state,  $C_u$  and  $C_l$  are the population probability amplitudes of the upper state and lower state of the *whole* system, respectively. In view of Eqs. (6), (9), (4) and the integral relationship

$$\text{Im } G_{\alpha\beta}(\mathbf{r}, \mathbf{r}', \omega) =$$

$$\frac{4\pi}{c} k \int d\mathbf{R} \text{Re} \sigma_{zz}(\mathbf{R}, \omega) G_{\alpha z}(\mathbf{r}, \mathbf{R}, \omega) G_{\beta z}^*(\mathbf{r}', \mathbf{R}, \omega)$$

(which is nothing but a particular case of the general 3D Green tensor integral relationship rigorously proven in Ref. [6] with Eq. (3) taken into account), the Schrödinger equation with the Hamiltonian (5) and wave function (11) yields the following evolution law for the population probability amplitude of the upper state of the system

$$C_u(\tau) = 1 + \int_0^\tau K(\tau - \tau') C_u(\tau') d\tau', \quad (12)$$

$$K(\tau - \tau') = \frac{\hbar \Gamma_0(x_A)}{4\pi x_A^3 \gamma_0} \int_0^\infty dx x^3 \xi(x) \frac{e^{-i(x - x_A)(\tau - \tau')} - 1}{i(x - x_A)}. \quad (13)$$

Here,

$$x = \frac{\hbar \omega}{2\gamma_0} \quad \text{and} \quad \tau = \frac{2\gamma_0 t}{\hbar} \quad (14)$$

are the dimensionless frequency and time, respectively, with  $\gamma_0 = 2.7$  eV being the carbon nearest neighbor hopping integral [29] appearing in the CN surface axial conductivity in Eq. (4),  $\Gamma_0$  is the rate of the *exponential*

atomic spontaneous decay in vacuum obtained from the general expression of the form [30, 31]

$$\Gamma(x) = \frac{8\pi d_z^2}{\hbar c^2} \left( \frac{2\gamma_0 x}{\hbar} \right)^2 \text{Im} G_{zz}(\mathbf{r}_A, \mathbf{r}_A, x) \quad (15)$$

by substituting

$$\text{Im} G_{zz}^v(\mathbf{r}_A, \mathbf{r}_A, x) = \frac{1}{6\pi c} \frac{2\gamma_0 x}{\hbar} \quad (16)$$

for the vacuum imaginary Green tensor [32]. The function  $\xi(x)$  is the relative density (with respect to vacuum) of photonic states near the CN given for  $r_A > R_{cn}$  (see Appendix B) by

$$\xi(x) = \frac{\Gamma(x)}{\Gamma_0(x)} = 1 + \frac{3}{\pi} \text{Im} \sum_{p=-\infty}^{\infty} \quad (17)$$

$$\int_C \frac{dy s(R_{cn}, x) v(y)^4 I_p^2[v(y)u(R_{cn})x] K_p^2[v(y)u(r_A)x]}{1 + s(R_{cn}, x) v(y)^2 I_p[v(y)u(R_{cn})x] K_p[v(y)u(R_{cn})x]},$$

where  $I_p$  and  $K_p$  are the modified cylindric Bessel functions,  $v(y) = \sqrt{y^2 - 1}$ ,  $u(r) = 2\gamma_0 r / \hbar c$ , and  $s(R_{cn}, x) = 2i\alpha u(R_{cn})x \bar{\sigma}_{zz}(R_{cn}, x)$  with  $\bar{\sigma}_{zz} = 2\pi\hbar\sigma_{zz}/e^2$  being the dimensionless conductivity and  $\alpha = e^2/\hbar c = 1/137$  representing the fine-structure constant. The integration contour  $C$  goes along the real axis of the complex plane and envelopes the branch points  $y = \pm 1$  of the function  $v(y)$  in the integrand from below and from above, respectively. For  $r_A < R_{cn}$ , Eq. (17) is modified by the simple replacement  $r_A \leftrightarrow R_{cn}$  in the Bessel function arguments in the numerator of the integrand. Note the divergence of  $\xi(x)$  at  $r_A = R_{cn}$ , i. e. when the atom is located right on the CN surface. The point is that the CN dielectric tensor longitudinal component  $\epsilon_{zz}$  [which, according to Eq. (3), is responsible for the surface axial conductivity  $\sigma_{zz}$  in Eq. (17)] is obtained as a result of a standard procedure of *physical* averaging a local electromagnetic field over the two spatial directions in the graphene plane [33]. Such averaging does not assume extrinsic atoms on the graphene surface. To take them into consideration the averaging procedure must be modified. Thus, the applicability domain of our model is restricted by the condition

$$|r_A - R_{cn}| > a, \quad (18)$$

where  $a = 1.42 \text{ \AA}$  is a graphene interatomic distance [29].

Eq. (12) is a well-known Volterra integral equation of the second kind. In our case, it describes the spontaneous decay dynamics of the excited two-level atom in the vicinity of the CN. All the CN parameters that are relevant for the spontaneous decay are contained in the relative density of photonic states (17) appearing in the kernel (13). The density of photonic states is, in turn, determined by the imaginary classical Green tensor of the CN-modified electromagnetic field via  $\Gamma(x)$  given by Eq. (15).

### III. QUALITATIVE ANALYSIS

In this Section we will qualitatively analyze the time dynamics of the upper state population probability  $C_u(\tau)$  in terms of two different approximations admitting analytical solutions of the evolution problem (12), (13). They are the Markovian approximation and the single-resonance approximation of the relative density  $\xi(x)$  of photonic states in the vicinity of the CN.

#### 1. Markovian approximation

In the case where the Markovian approximation is applicable, or, in other words, when the atom-field coupling strength is weak enough for atomic motion memory effects to be insignificant, so that they may be neglected, the time-dependent factor in the kernel (13) may be replaced by its long-time approximation

$$\frac{e^{-i(x-x_A)(\tau-\tau')} - 1}{i(x-x_A)} \rightarrow -\pi\delta(x-x_A) + i\mathcal{P}\frac{1}{x-x_A}$$

( $\mathcal{P}$  denotes a principal value). Then, in view of Eq. (17), the kernel becomes

$$K(\tau - \tau') = -\frac{\hbar\Gamma(x_A)}{4\gamma_0} + i\Delta(x_A)$$

with

$$\Delta(x_A) = \frac{\hbar\Gamma_0(x_A)}{4\gamma_0\pi x_A^3} \mathcal{P} \int_0^\infty dx x^3 \frac{\xi(x)}{x - x_A},$$

and Eq. (12) yields

$$C_u(\tau) = \exp \left\{ \left[ -\frac{\hbar\Gamma(x_A)}{4\gamma_0} + i\Delta(x_A) \right] \tau \right\} \quad (19)$$

— the exponential decay dynamics of the [shifted by  $\Delta(x_A)$ ] upper atomic level with the rate  $\Gamma(x_A)$ . This case was analyzed in Ref. [34].

#### 2. Single-resonance approximation of the relative density of photonic states

Another approximation that admits an analytical solution of the evolution problem (12), (13) is a single-resonance approximation. Suppose that at  $x = x_r$  the photonic density of states  $\xi(x)$  has a sharp peak of half-width-at-half-maximum  $\delta x_r$ . For all  $x$  in the vicinity of  $x_r$ , the shape of  $\xi(x)$  may then be roughly approximated by the Lorentzian function of the form

$$\xi(x) \approx \frac{\xi(x_r)\delta x_r^2}{(x - x_r)^2 + \delta x_r^2}.$$

The kernel (13) is then easily calculated analytically to give

$$K(\tau - \tau') \approx \frac{\hbar\Gamma(x_r)}{2\gamma_0} \frac{\delta x_r}{2}$$

$$\times \frac{\exp[-i(x_r - i\delta x_r - x_A)(\tau - \tau') - 1]}{i(x_r - i\delta x_r - x_A)}, \quad \tau > \tau'.$$

Substituting this into Eq. (12) and making the differentiation of both sides of the resulting equation over time, followed by the change of the integration order and one more time differentiation, one straightforwardly arrives at a second order ordinary homogeneous differential equation

$$\ddot{C}_u(\tau) + i(x_r - i\delta x_r - x_A)\dot{C}_u(\tau) + (\Omega/2)^2 C_u(\tau) = 0,$$

where  $\Omega = \sqrt{2\delta x_r \hbar \Gamma(x_r)/2\gamma_0}$ , with the solution given for  $x_A \approx x_r$  by

$$C_u(\tau) \approx \frac{1}{2} \left( 1 + \frac{\delta x_r}{\sqrt{\delta x_r^2 - \Omega^2}} \right) \exp \left[ - \left( \delta x_r - \sqrt{\delta x_r^2 - \Omega^2} \right) \frac{\tau}{2} \right] + \frac{1}{2} \left( 1 - \frac{\delta x_r}{\sqrt{\delta x_r^2 - \Omega^2}} \right) \exp \left[ - \left( \delta x_r + \sqrt{\delta x_r^2 - \Omega^2} \right) \frac{\tau}{2} \right]. \quad (20)$$

This solution is approximately valid for those atomic transition frequencies  $x_A$  which are located in the vicinity of the photonic density-of-states resonances whatever the atom-field coupling strength is. In particular, if  $(\Omega/\delta x_r)^2 \ll 1$ , Eq. (20) yields the exponential decay of the upper atomic state population probability  $|C_u(\tau)|^2$  with the rate  $\hbar\Gamma(x_r)/2\gamma_0$  in full agreement with Eq. (19) obtained within the Markovian approximation for weak atom-field coupling. In the opposite case, when  $(\Omega/\delta x_r)^2 \gg 1$ , one has

$$|C_u(\tau)|^2 \approx e^{-\delta x_r \tau} \cos^2 \left( \frac{\Omega \tau}{2} \right),$$

and the decay of the upper atomic state population probability proceeds via damped Rabi oscillations. This is the principal signature of strong atom-field coupling which is beyond the Markovian approximation. Expressing  $\Gamma(x_r)$  in  $\Omega$  in terms of  $\xi(x_r)$  by means of Eq. (17) and using the approximation  $\Gamma_0(x) \approx \alpha^3 2\gamma_0 x/\hbar$  valid for hydrogen-like atoms [35], one may conveniently rewrite the strong atom-field coupling condition in the form

$$2\alpha^3 x_r \frac{\xi(x_r)}{\delta x_r} \gg 1, \quad (21)$$

from which it follows that the strong coupling regime is fostered by high and narrow resonances in the relative density of photonic states.

#### IV. NUMERICAL RESULTS AND DISCUSSION

To get beyond the Markovian and single-peak approximations, we have solved Eqs. (12) and (13) numerically. The *exact* time evolution of the upper state population probability  $|C_u(\tau)|^2$  was obtained for the atom placed [in a way that Eq. (18) was always satisfied] in the

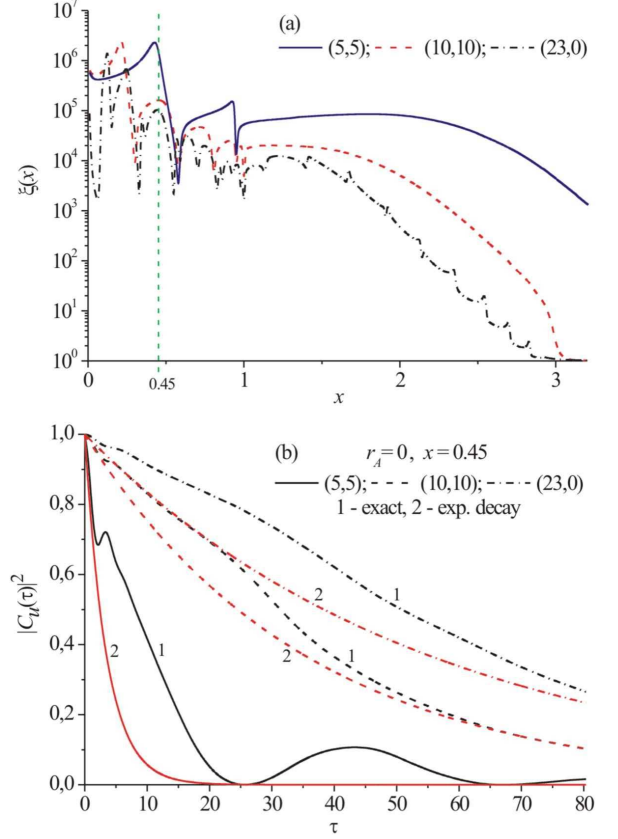


FIG. 2: (Color online) Relative density of photonic states (a) and upper-level spontaneous decay dynamics (b) for the atom in the center of different CNs. The atomic transition frequency is indicated by the dashed line in Fig. 2 (a).

center and near the wall inside, and at different distances outside achiral CNs of different radii. The relative density of photonic states  $\xi(x)$  in Eq. (13) was computed according to Eq. (17). The CN surface axial conductivity  $\sigma_{zz}$  appearing in Eq. (17) was calculated in the relaxation-time approximation with the relaxation time  $3 \times 10^{-12}$  s; the spatial dispersion of  $\sigma_{zz}$  was neglected [23]. The free-space spontaneous decay rate was approximated by the expression  $\Gamma_0(x) \approx \alpha^3 2\gamma_0 x/\hbar$  [35].

Figure 2 (a) presents  $\xi(x)$  for the atom in the center of the (5,5), (10,10) and (23,0) CNs. It is seen to decrease with increasing the CN radius, representing the decrease of the atom-field coupling strength as the atom moves away from the CN surface [34]. To calculate  $|C_u(\tau)|^2$  in this particular case, we have fixed  $x_A = 0.45$  (indicated by the vertical dashed line), firstly, because this transition is located within the visible light range  $0.305 < x < 0.574$ , secondly, because this is the approximate peak position of  $\xi(x)$  for all the three CNs. The functions  $|C_u(\tau)|^2$  calculated are shown in Figure 2 (b) in comparison with those obtained in the Markovian approximation yielding the exponential decay. The actual spontaneous decay dynamics is clearly seen to be non-exponential. For the

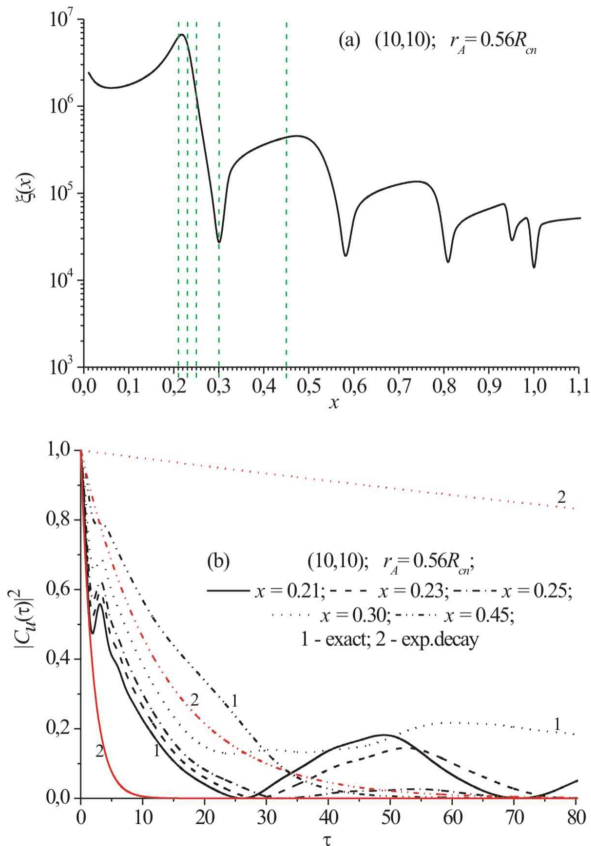


FIG. 3: (Color online) (a) Fragment of the relative density of photonic states for the atom inside the (10,10) CN at distance of 3 Å from the wall (the situation observed experimentally for Cs in Ref. [18]). (b) The upper-level spontaneous decay dynamics for different atomic transition frequencies [indicated by the dashed lines in Fig. 3 (a)] in this particular case.

small radius (5,5) CN, Rabi oscillations are observed, indicating a *strong* atom-field coupling regime related to *strong* non-Markovian memory effects. Eq. (21) is satisfied in this case. With increasing the CN radius, as the value of  $\xi(0.45)$  decreases, Eq. (21) ceases to be valid and the decay dynamics approaches the exponential one with the decay rate enhanced by several orders of magnitude compared with that in free space. Note that, though the distance from the atom to the CN surface is larger for the (23,0) CN than for the (10,10) CN, the deviation of the actual decay dynamics from the exponential one is larger for the (23,0) CN. This is an obvious consequence of the influence of a small neighboring peak in the (23,0) CN photonic density of states [Figure 2 (a)].

In Ref. [18], formation of Cs-encapsulating single-wall CNs was reported. In a particular case of the (10,10) CN, the stable Cs atom/ion position was observed to be at distance of 3 Å from the wall. We have simulated the spontaneous decay dynamics for a number of typical atomic transition frequencies for this case. Figure 3 (a) shows the density of photonic states and the five spe-

cific transition frequencies  $x_A$  (dashed lines) for which the functions  $|C_u(t)|^2$  presented in Figure 3 (b) were calculated. Rabi oscillations are clearly seen to occur in the vicinity of the highest peak ( $x_A \approx 0.22$ ) of the photonic density of states. Important is that they persist for large enough detuning values  $x_A \approx 0.21 \div 0.25$ . For  $x_A = 0.30$ , the density of photonic states has a dip, and the decay dynamics exhibits no Rabi oscillations, being strongly non-exponential nevertheless. For  $x_A = 0.45$ , the intensity of the peak of the photonic density of states is not large enough and the peak is too broad, so that strong atom-field coupling condition (21) is not satisfied and the decay dynamics is close to the exponential one.

Figure 4 (a) shows the density of photonic states for the atom outside the (9,0) CN at the different distances from its surface. The vertical dashed lines indicate the atomic transitions for which the functions  $|C_u(\tau)|^2$  in Figures 4 (b), (c), and (d) were calculated. The transitions  $x_A = 0.33$  and  $0.58$  are the positions of sharp peaks (at least for the shortest atom-surface distance), while  $x_A = 0.52$  is the position of a dip of the function  $\xi(x)$ . Very clear underdamped Rabi oscillations are seen for the shortest atom-surface distance at  $x_A = 0.33$  [Figure 4 (b)], indicating strong atom-field coupling with strong non-Markovity. For  $x_A = 0.58$  [Figure 4(d)], the value of  $\xi(0.58)$  is not large enough for strong atom-field coupling to occur, so that Eq. (21) is not fulfilled. As a consequence, the decay dynamics, being strongly non-exponential in general, exhibits no clear Rabi oscillations. For  $x_A = 0.52$  [Figure 4 (c)], though  $\xi(0.52)$  is comparatively small, the spontaneous decay dynamics is still non-exponential, approaching the exponential one only when the atom is far enough from the CN surface.

The reason for non-exponential spontaneous decay dynamics in all the cases considered is similar to that taking place in photonic crystals [9]. When the atom is closed enough to the CN surface, an absolute value of the relative density of photonic states is large and its frequency variation in the neighborhood of a specific atomic transition frequency essentially influences the time behavior of the kernel (13) of evolution equation (12). Physically, this means that the correlation time of the electromagnetic vacuum is not negligible on the time scale of the evolution of the atomic system, so that atomic motion memory effects are important and the Markovian approximation in the kernel (13) is inapplicable.

## V. CONCLUSIONS

The effects we predict will yield an additional structure in optical absorbance/reflectance spectra (see, e.g., [26, 27]) of atomically doped CNs in the vicinity of the energy of an atomic transition. Weak non-Markovity of the spontaneous decay (non-exponential decay with no Rabi oscillations) will cause an asymmetry of an optical spectral line-shape (similar to exciton optical absorption line-shape in quantum dots [36]). Strong non-Markovity of

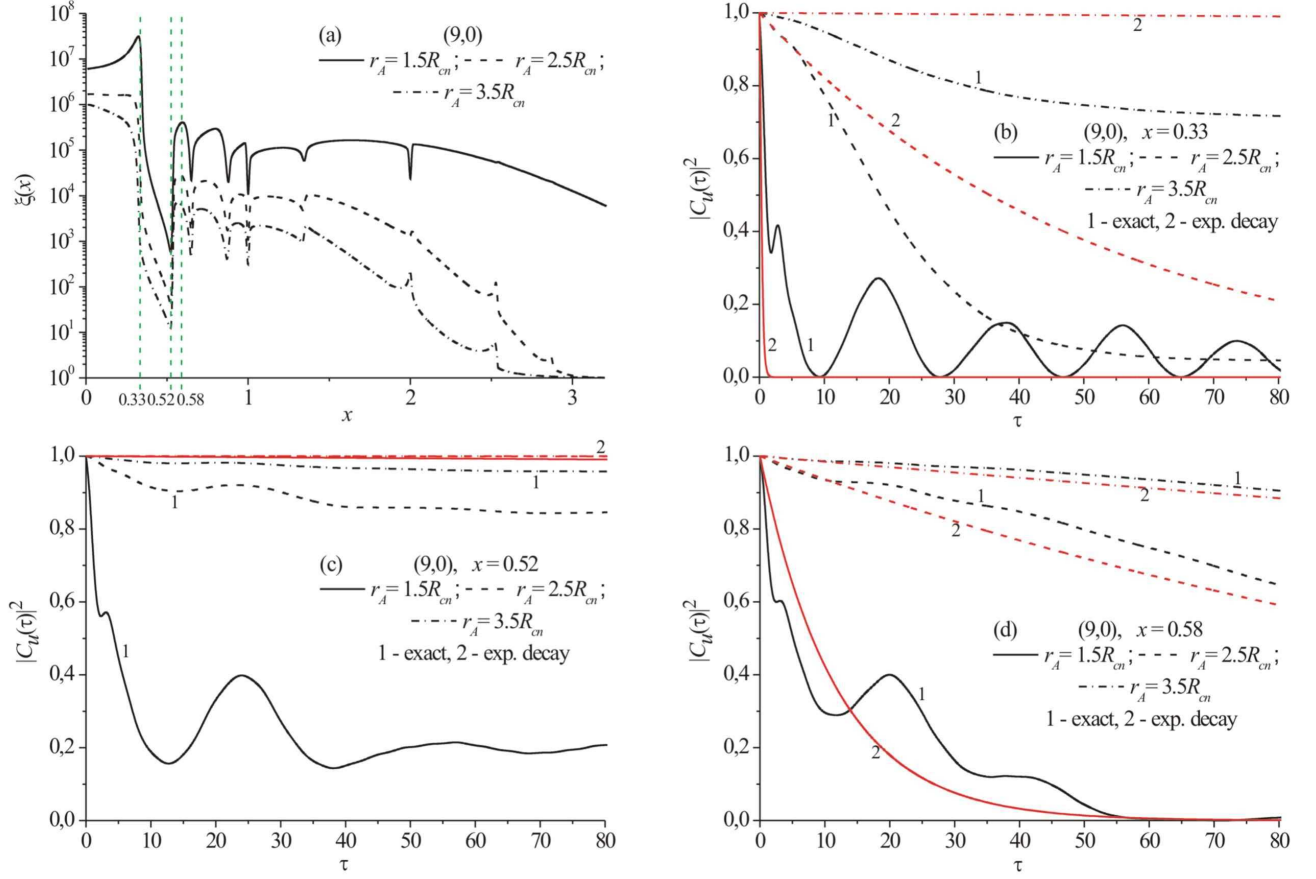


FIG. 4: (Color online) (a) Relative density of photonic states for the atom located at different distances outside the (9,0) CN. (b, c, d) Upper-level spontaneous decay dynamics for the three atomic transition frequencies [indicated by the dashed lines in Fig. 4 (a)] at different atom-nanotube-surface distances.

the spontaneous decay (non-exponential decay with fast Rabi oscillations) originates from strong atom-vacuum-field coupling with the upper state of the system splitted into two "dressed" states. This will yield a two-component structure of optical spectra similar to that observed for excitonic and intersubband electronic transitions in semiconductor quantum microcavities [21, 22].

Summarizing, we have developed the quantum theory of the spontaneous decay of an excited two-level atom near a carbon nanotube. In describing atom-field interaction, we followed an electromagnetic field quantization scheme developed for dispersing and absorbing media in Refs. [5, 6]. This quantization formalism was adopted by us for a particular case of an atom near an infinitely long single-wall CN. We derived the evolution equation of the upper state of the system and, by solving it numerically, demonstrated a strictly non-exponential spontaneous decay dynamics in the case where the atom is close enough to the CN surface. In certain cases, namely when the atom is close enough to the nanotube surface and the atomic transition frequency is in the vicinity of the resonance of the photonic density of states, the system exhibits vacuum-field Rabi oscillations, a principal sig-

nature of strong atom-vacuum-field coupling, — a result already detected for quasi-2D excitonic and intersubband electronic transitions in semiconductor quantum microcavities [21, 22] and never reported for atomically doped CNs so far. This is the result of strong non-Markovian memory effects arising from the rapid frequency variation of the photonic density of states near the nanotube. The non-exponential decay dynamics gives place to the exponential one if the atom moves away from the CN surface. Thus, the atom-vacuum-field coupling strength and the character of the spontaneous decay dynamics, respectively, may be controlled by changing the distance between the atom and CN surface by means of a proper preparation of atomically doped CNs. This opens routes for new challenging nanophotonics applications of atomically doped CN systems as various sources of coherent light emitted by dopant atoms.

Finally, we would like to emphasize a general character of the results we obtained. We have shown that similar to semiconductor microcavities [22] and photonic band-gap materials [9], carbon nanotubes may qualitatively change the character of atom-electromagnetic-field interaction, yielding strong atom-field coupling —

an important phenomenon necessary, e.g., for quantum information processing [37, 38, 39]. The present paper dealt with the simplest manifestation of this general phenomenon — vacuum-field Rabi oscillations in the atomic spontaneous decay dynamics near a single-wall carbon nanotube. However, similar manifestations of strong atom-field coupling may occur in many other atom-electromagnetic-field interaction processes in the presence of CNs, such as, e.g., dipole-dipole interaction between atoms by means of a vacuum photon exchange [40], or cascade spontaneous transitions in three-level atomic systems [41].

### Acknowledgments

We gratefully acknowledge numerous discussions with Dr. G.Ya. Slepyan and Prof. I.D. Feranchuk. I.B. thanks the Belgian OSTC. The work was performed within the framework of the Belgian PAI-P5/01 project.

### APPENDIX A: GREEN TENSOR OF A SINGLE-WALL CARBON NANOTUBE

The form of the classical electromagnetic field Green tensor in Eqs. (9) and (10) depends on the presence of external radiative sources (an atom in our case) and their position (inside or outside) with respect to a nanotube. Since the problem has a cylindric symmetry, we assign the orthonormal cylindric basis  $\{\mathbf{e}_r, \mathbf{e}_\varphi, \mathbf{e}_z\}$  (see Figure 1) in such a way that  $\mathbf{e}_z$  is directed along the nanotube axis and  $\mathbf{r}_A = r_A \mathbf{e}_r = \{r_A, 0, 0\}$ .

We use the representation

$$G_{\alpha z}(\mathbf{r}, \mathbf{r}_A, \omega) = \left( \frac{1}{k^2} \nabla_\alpha \nabla_z + \delta_{\alpha z} \right) g(\mathbf{r}, \mathbf{r}_A, \omega), \quad (\text{A1})$$

where  $\alpha = \{r, \varphi, z\}$  and the function  $g(\mathbf{r}, \mathbf{r}_A, \omega)$  is the Green function of the Helmholtz equation. Substituting Eq. (A1) into Eq. (10), one straightforwardly obtains

$$(\Delta + k^2) g(\mathbf{r}, \mathbf{r}_A, \omega) = -\delta(\mathbf{r} - \mathbf{r}_A) \quad (\text{A2})$$

with a known solution

$$g_0(\mathbf{r}, \mathbf{r}_A, \omega) = \frac{1}{4\pi} \frac{e^{ik|\mathbf{r}-\mathbf{r}_A|}}{|\mathbf{r} - \mathbf{r}_A|} \quad (\text{A3})$$

satisfying the radiation condition at infinity (see, e.g., [35]). In our case, however, the functions  $G_{\alpha z}(\mathbf{r}, \mathbf{r}_A, \omega)$  and  $g(\mathbf{r}, \mathbf{r}_A, \omega)$  are imposed one more set of boundary conditions. They are the boundary conditions on the surface of the CN. Using simple relations (valid for  $\mathbf{r} \neq \mathbf{r}_A$  under the Coulomb-gauge condition)

$$E_\alpha(\mathbf{r}, \omega) = ik G_{\alpha z}(\mathbf{r}, \mathbf{r}_A, \omega) \quad (\text{A4})$$

and

$$H_\alpha(\mathbf{r}, \omega) = -\frac{i}{k} \sum_{\beta, \gamma=r, \varphi, z} \epsilon_{\alpha\beta\gamma} \nabla_\beta E_\gamma(\mathbf{r}, \omega) \quad (\text{A5})$$

( $\epsilon_{\alpha\beta\gamma}$  is the totally antisymmetric unit tensor of rank 3), they can be derived from the classical electromagnetic field boundary conditions of the form

$$\underline{E}_\varphi|_{r=R_{cn}+0} - \underline{E}_\varphi|_{r=R_{cn}-0} = 0, \quad (\text{A6})$$

$$\underline{E}_z|_{r=R_{cn}+0} - \underline{E}_z|_{r=R_{cn}-0} = 0, \quad (\text{A7})$$

$$\underline{H}_\varphi|_{r=R_{cn}+0} - \underline{H}_\varphi|_{r=R_{cn}-0} = \frac{4\pi}{c} \sigma_{zz}(R_{cn}, \omega) \underline{E}_z|_{r=R_{cn}}, \quad (\text{A8})$$

$$\underline{H}_z|_{r=R_{cn}+0} - \underline{H}_z|_{r=R_{cn}-0} = 0 \quad (\text{A9})$$

(spatial dispersion neglected) obtained in Ref. [23].

Let  $r_A > R_{cn}$  (the atom outside the CN) to be specific. Then,  $g(\mathbf{r}, \mathbf{r}_A, \omega)$  may be represented in the form

$$g(\mathbf{r}, \mathbf{r}_A, \omega) = \begin{cases} g_0(\mathbf{r}, \mathbf{r}_A, \omega) + g^{(+)}(\mathbf{r}, \omega), & r > R_{cn} \\ g^{(-)}(\mathbf{r}, \omega), & r < R_{cn} \end{cases} \quad (\text{A10})$$

where  $g_0(\mathbf{r}, \mathbf{r}_A, \omega)$  is the point radiative atomic source function defined in Eq. (A3) and  $g^{(\pm)}(\mathbf{r}, \omega)$  are unknown nonsingular functions satisfying the homogeneous Helmholtz equation and the radiation conditions at infinity. We seek them using integral decompositions over the modified cylindric Bessel functions  $I_p$  and  $K_p$  as follows [42]

$$g^{(\pm)}(\mathbf{r}, \omega) = \sum_{p=-\infty}^{\infty} e^{ip\varphi} \int_C \left\{ \frac{A_p(h) K_p(vr)}{B_p(h) I_p(vr)} \right\} e^{ihz} dh \quad (\text{A11})$$

and

$$g_0(\mathbf{r}, \mathbf{r}_A, \omega) = \frac{1}{(2\pi)^2} \sum_{p=-\infty}^{\infty} e^{ip\varphi} \times \int_C I_p(vr) K_p(vr_A) e^{ihz} dh, \quad r_A \geq r, \quad (\text{A12})$$

where  $A_p(h)$  and  $B_p(h)$  are unknown functions to be found from the boundary conditions (A6)–(A9) in view of Eqs. (A1), (A4) and (A5),  $v = v(h, \omega) = \sqrt{h^2 - k^2}$ . The integration contour  $C$  goes along the real axis of the complex plane and envelopes the branch points  $\pm k$  from below and from above, respectively.

The boundary conditions (A6)–(A9) with Eqs. (A1), (A4) and (A5) taken into account yield the following two independent equations for the scalar Green function (A10)

$$g_0(\mathbf{r}, \mathbf{r}_A, \omega)|_{r=R_{cn}} + g^{(+)}(\mathbf{r}, \omega)|_{r=R_{cn}} = g^{(-)}(\mathbf{r}, \omega)|_{r=R_{cn}},$$

$$\frac{\partial g^{(+)}(\mathbf{r}, \omega)}{\partial r} \Big|_{r=R_{cn}} - \frac{\partial g^{(-)}(\mathbf{r}, \omega)}{\partial r} \Big|_{r=R_{cn}} +$$

$$\beta(\omega) \left( \frac{\partial^2}{\partial z^2} + k^2 \right) g^{(-)}(\mathbf{r}, \omega)|_{r=R_{cn}} = - \frac{\partial g_0(\mathbf{r}, \mathbf{r}_A, \omega)}{\partial r} \Big|_{r=R_{cn}},$$

where  $\beta(\omega) = 4\pi i \sigma_{zz}(R_{cn}, \omega)/\omega$ . Substituting the integral decompositions (A11) and (A12) into these equations, one obtains the set of two simultaneous algebraic equations for the functions  $A_p(h)$  and  $B_p(h)$ . The function  $A_p(h)$  we need (we only need the Green function in the region where the atom is located) is found by solving this set with the use of basic properties of cylindric Bessel functions (see, e.g., [43]). In so doing, one has

$$A_p(h) = -\frac{R_{cn}\beta(\omega)v^2I_p^2(vR_{cn})K_p(vr_A)}{(2\pi)^2[1+\beta(\omega)v^2R_{cn}I_p(vR_{cn})K_p(vR_{cn})]}.$$

These  $A_p(h)$ , being substituted into Eq. (A11), yield the function  $g^{(+)}(\mathbf{r}, \omega)$  sought. The latter one, in view of Eq. (A10), results in the scalar electromagnetic field Green function of the form

$$g(\mathbf{r}, \mathbf{r}_A, \omega) = g_0(\mathbf{r}, \mathbf{r}_A, \omega) - \frac{R_{cn}}{(2\pi)^2} \times \sum_{p=-\infty}^{\infty} e^{ip\varphi} \int_C \frac{\beta(\omega)v^2I_p^2(vR_{cn})K_p(vr_A)K_p(vr)}{1+\beta(\omega)v^2R_{cn}I_p(vR_{cn})K_p(vR_{cn})} e^{ihz} dh, \quad (\text{A13})$$

where  $r_A \geq r > R_{cn}$ . One may show in a similar way that the function  $g(\mathbf{r}, \mathbf{r}_A, \omega)$  for  $r \leq r_A < R_{cn}$  is obtained from Eq. (A13) by means of a simple symbol replacement  $I_p \leftrightarrow K_p$  in the numerator of the integrand.

Knowing  $g(\mathbf{r}, \mathbf{r}_A, \omega)$ , one may easily compute the components of the electromagnetic field Green tensor  $G_{\alpha\gamma}(\mathbf{r}, \mathbf{r}_A, \omega)$  according to Eq. (A1).

## APPENDIX B: DENSITY OF PHOTONIC STATES NEAR A SINGLE-WALL CARBON NANOTUBE

The relative density of photonic states in an atomic spontaneous decay process near a CN is defined by the

ratio [see Eqs. (14)–(17)]

$$\xi(\omega) = \frac{\text{Im } G_{zz}(\mathbf{r}_A, \mathbf{r}_A, \omega)}{\text{Im } G_{zz}^v(\mathbf{r}_A, \mathbf{r}_A, \omega)}, \quad (\text{B1})$$

where

$$G_{zz}(\mathbf{r}_A, \mathbf{r}_A, \omega) = \left( \frac{1}{k^2} \frac{\partial^2}{\partial z^2} + 1 \right) g(\mathbf{r}, \mathbf{r}_A, \omega)|_{\mathbf{r}=\mathbf{r}_A} \quad (\text{B2})$$

according to Eq. (A1),  $g(\mathbf{r}, \mathbf{r}_A, \omega)$  is given by Eq. (A13) for  $r_A \geq r > R_{cn}$  and by the same equation with the symbol replacement  $I_p \leftrightarrow K_p$  in the numerator of the integrand for  $r \leq r_A < R_{cn}$ .

Substituting Eq. (A13) into Eq. (B2), making differentiation and passing to the limit  $\mathbf{r} \rightarrow \mathbf{r}_A$ , followed by the substitution of the result into Eq. (B1), one has for  $r_A > R_{cn}$

$$\xi(\omega) = 1 + \frac{3R_{cn}}{2\pi k^3} \quad (\text{B3})$$

$$\times \text{Im} \sum_{p=-\infty}^{\infty} \int_C \frac{\beta(\omega)v^4I_p^2(vR_{cn})K_p^2(vr_A)}{1+R_{cn}\beta(\omega)v^2I_p(vR_{cn})K_p(vR_{cn})} dh.$$

For  $r_A < R_{cn}$ , Eq. (B3) is modified either by the symbol replacement  $I_p \leftrightarrow K_p$  or by the Bessel function argument replacement  $r_A \leftrightarrow R_{cn}$  in the numerator of the integrand. In dimensionless variables (14), Eq. (B3) is rewritten to give Eq. (17).

- 
- [1] E.M. Purcell, Phys. Rev. **69**, 681 (1946).
  - [2] J.D. Rarity and C. Weisbuch, *Microcavities and Photonic Bandgaps: Physics and Applications*, NATO ASI Series (Kluwer, Dordrecht, 1996), Vol. E324.
  - [3] M. Pelton and Y. Yamamoto, Phys. Rev. A **59**, 2418 (1999).
  - [4] J. Vučković, D. Fattal, C. Santori, G.S. Solomon, and Y. Yamamoto, Appl. Phys. Lett. **82**, 3596 (2003).
  - [5] H.T. Dung, L. Knöll, and D.-G. Welsch, Phys. Rev. A **62**, 053804 (2000) [and refs. therein].
  - [6] L. Knöll, S. Scheel, and D.-G. Welsch, in: *Coherence and Statistics of Photons and Atoms*, edited by J. Peřina (Wiley, New York, 2001).
  - [7] J.R. Buck and H.J. Kimble, Phys. Rev. A **67**, 033806 (2003).
  - [8] V.V. Klimov and M. Ducloy, e-print: physics/0206048.
  - [9] M. Florescu and S. John, Phys. Rev. A **64**, 033801 (2001).
  - [10] M. Sugawara, Phys. Rev. B **51**, 10743 (1995).
  - [11] H. Schniepp and V. Sandoghdar, Phys. Rev. Lett. **89**, 257403 (2002).
  - [12] E.P. Petrov, V.N. Bogomolov, I.I. Kalosha, and S.V. Gaponenko, Phys. Rev. Lett. **81**, 77 (1998).
  - [13] B. Gayral, J.-M. Gérard, B. Sermage, A. Lemaître, and C. Dupuis, Appl. Phys. Lett. **78**, 2828 (2001).
  - [14] M.S. Dresselhaus, G. Dresselhaus, and P.C. Eklund, *Science of Fullerenes and Carbon Nanotubes* (Academic Press, New York, 1996).
  - [15] H. Dai, Surf. Sci. **500**, 218 (2002).
  - [16] R.H. Baughman, A.A. Zakhidov, and W.A. de Heer, Science **297**, 787, 2002.
  - [17] L. Duclaux, Carbon **40**, 1751 (2002).
  - [18] G.-H. Jeong, A.A. Farajian, R. Hatakeyama, T. Hirata *et al.*, Phys. Rev. B **68**, 075410 (2003).
  - [19] H. Shimoda, B. Gao, X.P. Tang, A. Kleinhammes *et al.*, Phys. Rev. Lett. **88**, 015502 (2002).
  - [20] L. Allen and J. H. Eberly, *Optical Resonance and Two-*

- Level Atoms* (Wiley, New York, 1975).
- [21] C. Weisbuch, M. Nishioka, A. Ishikawa, and Y. Arakawa, Phys. Rev. Lett. **69**, 3314 (1992).
  - [22] D. Dini, R. Köhler, A. Tredicucci, G. Biasiol, and L. Sorba, Phys. Rev. Lett. **90**, 116401 (2003).
  - [23] G.Ya. Slepyan, S.A. Maksimenko, A. Lakhtakia, O. Yevtushenko, and A.V. Gusakov, Phys. Rev. B **60**, 17136 (1999).
  - [24] S. Tasaki, K. Maekawa, and T. Yamabe, Phys. Rev. B **57**, 9301 (1998).
  - [25] A. Jorio, A.G. Souza Filho, V.W. Brar, A.K. Swan *et al.*, Phys. Rev. B **65**, 121402R (2002).
  - [26] Z.M. Li, Z.K. Tang, H.J. Liu, N. Wang *et al.*, Phys. Rev. Lett. **87**, 127401 (2001).
  - [27] A.G. Marinopoulos, L. Reining, A. Rubio, and N. Vast, Phys. Rev. Lett. **91**, 046402 (2003).
  - [28] W. Vogel, D.-G. Welsch and S. Wallentowitz, *Quantum Optics: an Introduction* (Wiley-VCH, New York, 2001).
  - [29] P.R. Wallace, Phys. Rev. **71**, 622 (1947).
  - [30] S.M. Barnett, B. Huttner, and R. Loudon, Phys. Rev. Lett. **68**, 3698 (1992).
  - [31] G.S. Agarwal, Phys. Rev. A **42**, 1475 (1975).
  - [32] A.A. Abrikosov, L.P. Gorkov, and I.E. Dzyaloshinski, *Methods of Quantum Field Theory in Statistical Physics* (Dover, New York, 1975).
  - [33] L. Henrard and Ph. Lambin, J. Phys. B **29**, 5127 (1996).
  - [34] I.V. Bondarev, G.Ya.Slepyan, and S.A. Maksimenko, Phys. Rev. Lett. **89**, 115504 (2002).
  - [35] A.S. Davydov, *Quantum Mechanics* (NEO, Ann Arbor, MI, 1967).
  - [36] I.V. Bondarev, S.A. Maksimenko, G.Ya.Slepyan, I.L.Krestnikov, and A. Hoffmann, Phys. Rev. B **68**, 073310 (2003).
  - [37] J.M. Raimond, M. Brune, and S. Haroche, Rev. Mod. Phys. **73**, 565 (2001).
  - [38] A. Zrenner, E. Beham, S. Stuffer, F. Findeis, M. Bichler, and G. Abstreiter, Nature **418**, 612 (2002).
  - [39] X. Li, Y. Wu, D. Steel, D. Gammon *et al.*, Science **301**, 809 (2003).
  - [40] G.S. Agarwal and S. Dutta Gupta, Phys. Rev. A **57**, 667 (1998).
  - [41] B.J. Dalton and B.M. Garraway, Phys. Rev. A **68**, 033809 (2003).
  - [42] J.D. Jackson, *Classical Electrodynamics* (Wiley, New York, 1975).
  - [43] *Handbook of Mathematical Functions*, eds. M. Abramowitz and I.A. Stegun (Dover, New York, 1972).